

# DETECTION AND MONITORING OF TWO DUST STORM EVENTS BY MULTISPECTRAL MODIS IMAGES

Mehta Prachi S.<sup>1</sup> and Kunte Pravin D.\*<sup>2</sup>

1. Center for Environmental Planning and Technology, Ahmadabad, Gujarat (INDIA)
2. CSIR-National Institute of Oceanography, Dona Paula, Goa (INDIA)

Received January 14, 2014

Accepted May 20, 2014

## ABSTRACT

During a dust storm event, loose sand/dust from a dry area is picked up and tossed into the air. These particles get together and form a layer of dust. These layers carry large amount of dust from one place to another and affect global meteorological conditions. The present study addresses detection, migration, altitude measurements and spread of two intense dust storm outbreaks events over the Arabian Sea region using multi-satellite observations. The first event occurred on 15<sup>th</sup> October 2008 when intense plumes of dust blew over Arabian Sea from the south coast of Pakistan. The second event of the dust storm originated in Arabian desert on March 25<sup>th</sup>. The plume extended hundreds of kilometers across southern shore of Oman, over Arabian Sea to the coast of Pakistan. The dust storm lasted over the Arabian Sea till 30<sup>th</sup> March. MODIS sensors on both Terra and Aqua Satellites captured images of both events. From the difference in emissive/transmissive nature of the mineral aerosol, suspended dust is distinguished from the ground scene. The algorithms based on split window brightness temperature difference, relations among reflectance at different wavelengths and their ratios and normalized difference indices like Normalized Difference Dust Index (NDDI), Normalized Difference Vegetation Index (NDVI) and Modified Normalized Difference Vegetation Index (MNDVI) were utilized to map the dust events. Selection of an appropriate algorithm is based on nature of the underlying surface, density of dust plumes, presence of clouds, geographic region of the event and time of image acquisition. CALIPSO LiDAR Data is analyzed over the footprint of CALIPSO (Cloud –Aerosol, LiDAR and Infrared Pathfinder Satellite Observation) on the MODIS (Moderate Resolution Imaging Spectroradiometer) scene and altitude of the dust storm is estimated from a profile of total attenuated backscatter. CALIPSO LiDAR measurements are also used to validate the observations. In this study, two dust storm events with dissimilar origins have been studied to evaluate different techniques of dust detection.

**Key Words :** Remote sensing, Dust pollution, MODIS, CALIPSO, NDVI, MNDVI

## INTRODUCTION

Satellite-based measurements for monitoring these atmospheric constituents are a viable proposition since ground-based measurements are limited in space and time.<sup>1,2</sup> Due to variability in emissive/transmissive nature of the mineral aerosol the ability of satellite data to detect dust plume is dependent of several factors. Different algorithms, spectral bands and thresholds are to be determined based on underlying land/ocean surface, density of dust plumes, presence of clouds, geographic region of the event and time of data acquisition. This

study compares various dust enhancement methodologies for visual analysis of dust and dust detection algorithms for determining whether a pixel is dusty or not. The objective is to establish which methods are most suitable under specific conditions. Advantages and drawbacks of each method are recognized as we evaluate these methods on two dust storm events of different origins over the Arabian Sea. In addition to this, CALIOP LiDAR total attenuated backscatter profile could be used to validate the results and measure the altitude of the dust storm. An assessment of brightness temperature difference along the CALIPSO footprint<sup>3</sup> with Vertical Feature Mask (VFM)

\*Author for correspondence

and aerosol subtype profile demonstrates the effect of pollutants and smoke on the brightness temperature difference of dust aerosols. The present study is about two dust storm events over Arabian Sea. This area has been selected because dust storm happening over Arabian Sea affects many countries of Middle East and Indian subcontinent like Saudi Arabia, Yemen, Oman, Kuwait, Bahrain,

Qatar, UAE, Iraq, Iran, Pakistan, Afghanistan and India. The first event is from mid October 2008 when plumes of dust blew from the South coast of Pakistan (**Fig. 1**). The dust was suspended into air when MODIS sensor on the Terra Satellite captured the image (**Fig. 2**) in the morning overpass. The intensified could be seen in the afternoon overpass of Aqua (**Fig. 3**) over the same region.

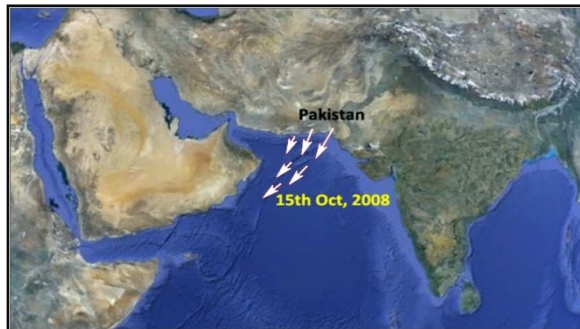


**Fig. 1 :** 15<sup>th</sup> Oct, 2008 dust storm - transport of dust

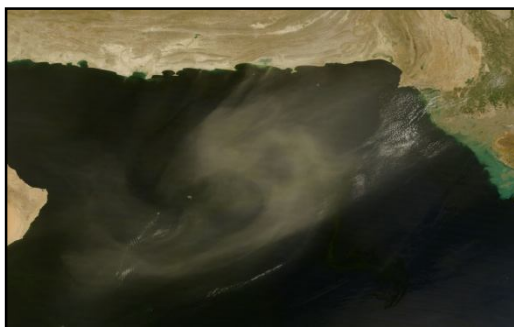


**Fig. 2 :** 15<sup>th</sup> Oct, 2008 Terra MODIS image



**Fig. 3 :** 15<sup>th</sup> Oct, 2008, Aqua MODIS image

The second event is of the dust storm originated in Arabian Desert on March 25<sup>th</sup> (**Fig. 4** and **Fig. 5**). The plume extended across hundreds of kilometers from Southern shores

of Oman to the coast of Pakistan (**Fig. 6**). The layer of dust from the powerful storm could be seen over the Arabian Sea (**Fig. 7**) till 30<sup>th</sup> March.

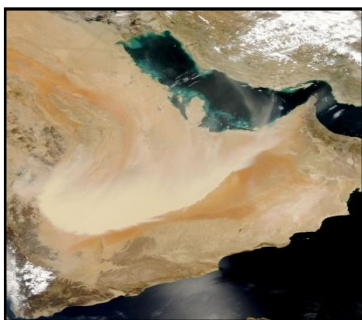


**Fig. 4 :** 25<sup>th</sup> March, 2011  
Aqua MODIS image

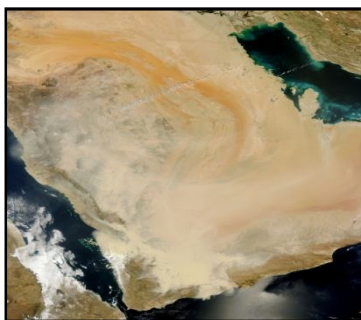


**Fig. 5 :** 27<sup>th</sup> March, 2011  
Terra MODIS image

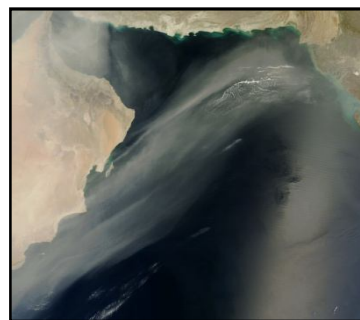


**Fig. 6 :** 30<sup>th</sup> March, 2011  
Terra MODIS image



Fig. 7 : March 2011 dust storm - transport of dust

**MATERIAL AND METHODS**

**MODIS data processing**

The dust detection methods discussed in this study can be used with any multi-channel imagers with channels at (or close to) 0.47 (blue), 0.55 (green), 0.64 (red), 0.86 (IR), 1.38 (shortwave water vapor absorption band), 2.26, 3.9, 11.0 and 12.0  $\mu\text{m}$ . These methods are demonstrated using MODIS L1B processed by software HYDRA (HYperspectral viewer for Development of Research Application).

**True color image**

Channels 1, 4 and 3 respectively are the red,

green and blue wavelengths with 250m spatial resolutions. This composite gives true color image (Fig. 8). The dust absorbs blue wavelengths and appears yellowish brown. Clouds are spectrally neutral and appear white in true color image (Fig. 9).

**Pseudo color image**

By using channels 7, 2 and 1 for red, green and blue guns respectively, we get a pseudo color technique is applied to enhance the color composite (Fig. 10) which helps us in distinguishing among clouds, sunglint, and dust to some extent. Suitable histogram stretch contrast (Fig. 11).

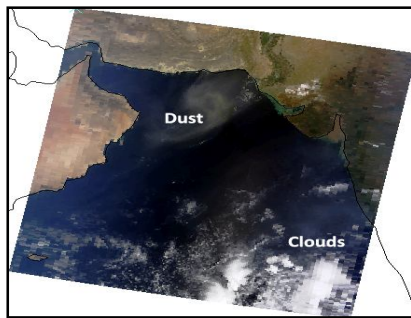


Fig. 8 : True color RGB of 2008 dust storm

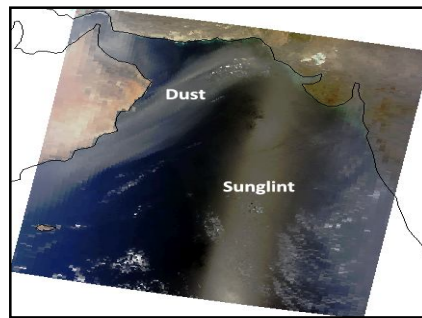


Fig. 9 : True color RGB of 2011 dust storm

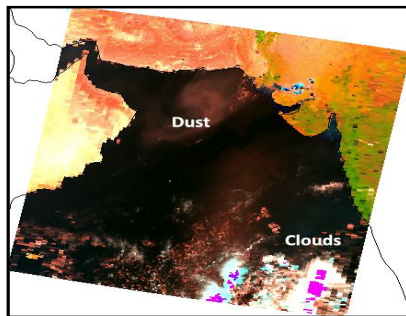


Fig. 10 : Pseudo color RGB of 2008 dust storm

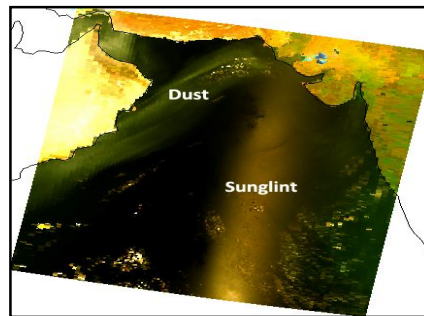
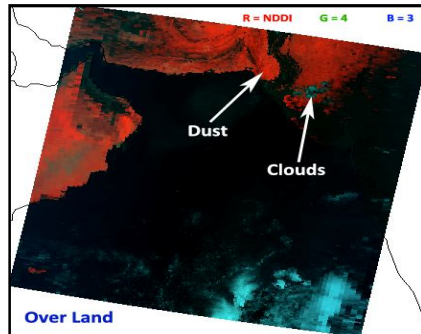


Fig. 11 : Pseudo color RGB of 2011 dust storm

**Enhanced red RGB**

Miller<sup>4</sup> suggested that if red gun of the RGB composite for an image is replaced with a channel or linear composition of channels that are characteristic to dust, it can produce an

image that enhances dust (Fig. 12 and Fig. 13). For dust detection over land and ocean, NDDI and brightness temperature difference between 12 and 11 $\mu$ m BTD (12, 11) are respectively suitable as red gun (Fig. 14 and Fig. 15).



**Fig. 12 :** Enhanced dust over land (2008)

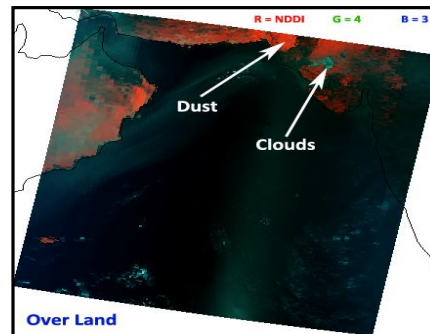


**Fig. 13 :** Enhanced dust over land (2011)

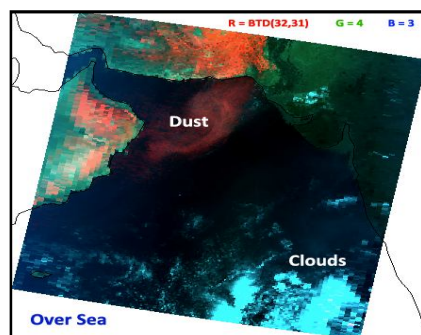


**Fig. 14 :** Enhanced dust over ocean (2008)

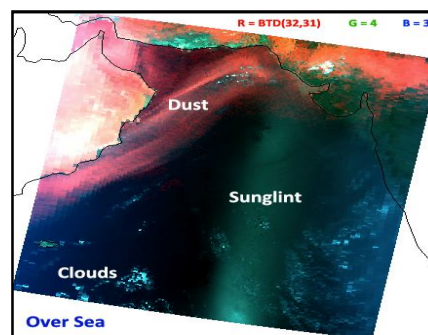


**Fig. 15 :** Enhanced dust over ocean (2011)

**Dust detection algorithms**

Zhao<sup>5</sup> et al. has demonstrated the following dust detection tests. There are different schemes for dust detection over land and ocean.

**A . Dust detection over land****1. Good data test for BT and R**

$R_{0.47\mu m}, R_{0.64\mu m}, R_{0.86\mu m}, R_{1.38\mu m} > 0$   
 $BT_{3.9\mu m}, BT_{11\mu m}, BT_{12\mu m} > 0K$

Any negative value in reflectance or brightness temperature shows error in data. Such data should not be used.

**2. BTD and R tests**

$BT_{11\mu m} - BT_{12\mu m} \leq -0.5K$  &  $BT_{3.9\mu m} - BT_{11\mu m} \geq 20K$ , and  $R_{1.38\mu m} < 0.055$

Screen for pixels that are water cloud free. If these conditions are not met, then the pixels are cloudy and further dust detection tests need not be carried out.

**3. Dust test**

If  $BT_{3.9\mu m} - BT_{11\mu m} \geq 25K$  then dust

If  $MNDVI < 0.08$  and  $Rat_2 > 0.005$  then dust

Dust reflects solar energy at 3.9 $\mu$ m so during the day brightness temperature difference with BT11 $\mu$ m is significant. Depending on the time of data acquisition, 25K threshold for the BTD (3.9, 11) might have to be lowered down even till 15K in case of layer of dust that is not very dense. MNDVI gives a more accurate result in this case. MNDVI is a modified normalized difference index that involves Red (~0.64 $\mu$ m) and reflective Infrared (~0.86 $\mu$ m) wavelengths. This can be useful for detection of dust over semi-arid surface with small amounts of vegetation. Moreover dust absorbs blue (~0.47 $\mu$ m) wavelength. Therefore the index  $Rat_2$  that is dependent on blue wavelength can be used effectively.



**4. Thick dust test**

$$BT_{11\mu\text{m}} - BT_{12\mu\text{m}} \leq -0.5\text{K} \ \& \ BT_{3.9\mu\text{m}} - BT_{11\mu\text{m}} \geq 25\text{K} \ \text{and} \ R_{1.38\mu\text{m}} < 0.035$$

$$\text{MNDVI} < 0.2$$

Higher threshold values are applied for separation of thick dust from the background. There is a possibility that there may not be any pixels in the image that pass this test. Many types of aerosols have strong spectral variation in 8-10 $\mu\text{m}$  and 10-12 $\mu\text{m}$  regions. This (8-14 $\mu\text{m}$ ) is also an infrared atmospheric window region i.e., the atmosphere is fairly transparent and causes no absorption or re-emission. Therefore, satellite radiance measurements in these wavelengths show favorable results for aerosol detection. Dust absorbs more radiation at 12 $\mu\text{m}$  than 11 $\mu\text{m}$ , which causes BT<sub>D</sub> (11, 12) to become negative. The 1.38 $\mu\text{m}$  channel is located in water vapor absorption band. If there are very dense clouds in the scene, it picks up dust signature as clear sky.

**B. Dust detection over ocean**

Dust detection over ocean is not performed over sea ice or in the presence of higher ice clouds. The specific tests currently implemented are as follows :

**1. Good data test**

$$R_{0.47\mu\text{m}}, R_{0.64\mu\text{m}}, R_{0.86\mu\text{m}} > 0$$

$$BT_{3.9\mu\text{m}}, BT_{11\mu\text{m}}, BT_{12\mu\text{m}} > 0\text{K}$$

Negative values for any of these parameters indicate invalid data. Such data should not be used for analysis.

**2. BT<sub>D</sub> and R tests plus uniformity texture tests**

$$4\text{K} < BT_{3.9\mu\text{m}} - BT_{11\mu\text{m}} \leq 20\text{K}$$

$$R_{0.47\mu\text{m}} \leq 0.3$$

$$\text{Mean}R_{0.86\mu\text{m}} > 0 \ \text{and} \ \text{Std}R_{0.86\mu\text{m}} \leq 0.005$$

(3 × 3 pixels) (identify water cloud)

The brightness temperature difference test separates dust from clouds. Dust is less reflective than clouds in blue wavelengths (~0.47  $\mu\text{m}$ ) and its texture is more uniform than the texture of clouds (standard deviation of 3 × 3 pixels is less).

**3. Dust test**

$$\text{If } BT_{11\mu\text{m}} - BT_{12\mu\text{m}} < 0.1\text{K} \ \text{and} \ -0.3 \leq \text{NDVI} \leq 0 \ \text{then dust}$$

$$\text{If } R_{0.47\mu\text{m}}/R_{0.64\mu\text{m}} < 1.2 \ \text{then dust}$$

$$\text{If } BT_{3.9\mu\text{m}} - BT_{11\mu\text{m}} > 10\text{K} \ \text{and} \ BT_{11\mu\text{m}} - BT_{12\mu\text{m}} < -0.1\text{K} \ \text{then dust}$$

Airborne dust causes a depression in  $BT_{11\mu\text{m}} -$

$BT_{12\mu\text{m}}$  value. Therefore it is useful in detecting dust plumes. However the split window difference can also lead to false positive tests so it is used in conjunction with NDVI-type test for the pixel. Clear sky tends to reflect more in 0.47  $\mu\text{m}$  than 0.64  $\mu\text{m}$  compared to dust particles. Therefore a threshold of 1.2 for that ratio can be set for dust. Similar to dust detection over land, low level clouds can have a negative split window brightness temperature difference. Therefore additional tests ( $BT_{3.9\mu\text{m}} - BT_{11\mu\text{m}} > 10\text{K}$  and  $BT_{11\mu\text{m}} - BT_{12\mu\text{m}} < -0.1\text{K}$ ) applied to attempt reducing cloud-contaminated pixels.

**4. Thick dust test**

$$BT_{3.9\mu\text{m}} - BT_{11\mu\text{m}} > 20\text{K} \ (\text{define potential thick dust regime})$$

$$\text{If } BT_{11\mu\text{m}} - BT_{12\mu\text{m}} \leq 0\text{K} \ \text{and} \ -0.3 \leq \text{NDVI} \leq 0.05 \ \text{then heavy dust}$$

The heavy dust test is similar to the heavy dust test over the land. Two conditions mentioned above indicate presence of optically thick dust. Similar to the tests of heavy dust over land, two conditions that indicate the presence of optically thick dust over ocean are employed. The first part of the test associated with BT<sub>D</sub> is the ocean version of the split window IR detection technique for heavy dust. The second part of the test associated with NDVI is similar to the detection of non-thick dust, which is used to reduce the false detection in the split window test.<sup>5</sup>

**CALIOP data usage**

Level-1 product of CALIOP has total attenuated backscatter profile. X-axis of CALIOP data shows distance along the orbit track. Y-axis is the altitude. LiDAR sees through thin clouds but cannot penetrate through thick clouds. The dark region below the thin cloud region is the area where no signal reached and therefore no information is available.

Formations at high altitude usually indicate clouds and they have higher values (grey region on the color scale) of total attenuated backscatter (**Fig. 16**). Dust and other aerosols have lower total attenuated backscatter (yellow region on the color scale). Clear sky has the least total attenuated backscatter (dark blue region). Light blue, green colors on the color scale could be thin clouds through which LiDAR has passed through.

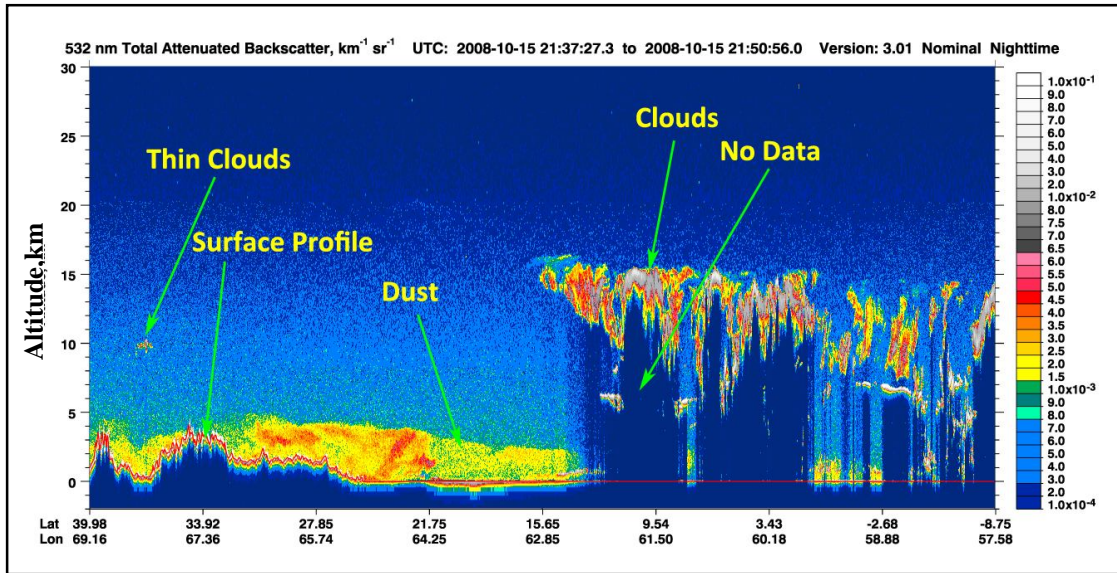


Fig. 16 : Interpreting a total attenuated backscatter profile

The higher levels of processed products<sup>3</sup> contain Vertical Feature Mask (VFM) and aerosol subtype among others (Fig. 17). They give further information about the types of aerosols. In illustrations below (Fig. 17 and Fig. 18), CALIOP attenuated backscattering signal profile at 532 nm is overlaid over

MODIS image and it shows the presence and altitude of the dust particles over the surface. Heavy aerosol over the Arabian Sea can be seen floating at the heights of 2-3 km. The clouds can be seen floating at the height of 7-13 km over the ocean in the 2008 event image (Fig. 17).

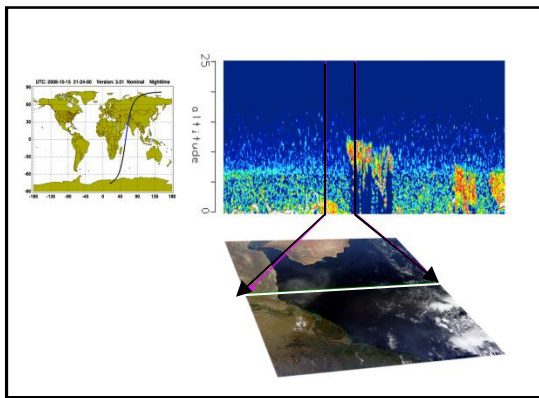


Fig. 17 : Overlay of CALIOP profile on MODIS image (2008)

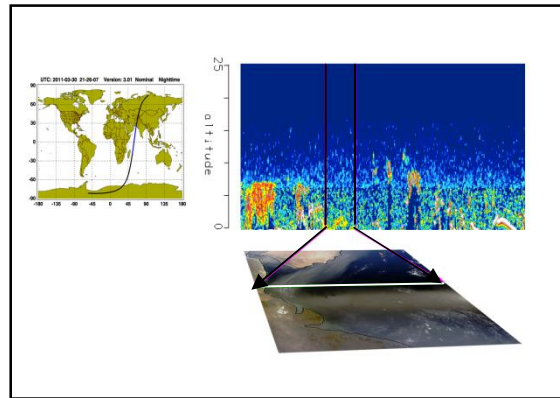


Fig. 18 : Overlay of CALIOP profile on MODIS image (2011)

**Verification of aerosol subtypes by MODIS brightness temperature difference**

As clouds and dust have difference in brightness temperature difference in thermal spectrum at 12 μm and 11 μm wavelengths, BTD (11,12) can be used to differentiate between the two. Usually BTD (11,12) are positive for clouds and negative for dust aerosol.<sup>6</sup> The overlapped area between both the

datasets is the CALIPSO path. The values of BTD (11,12) along the path can be either greater than or equal to zero or less than zero. If the values are less than 0, they can be identified as dust aerosol.

Fig. 19 and Fig. 20 show MODIS BTD (11, 12) values along the CALIOP path compared with the Vertical Feature Mask. In VFMs, parts of the region classified as aerosol have

BTD (11, 12) values above zero. This indicates that it comprises of something more than just dust. The aerosol subtype profile can reveal more information about it. Fig. 21 shows that the region that has higher values of BTD (11,

12) is polluted dust. Fig. 22 shows that the region that has higher values of BTD (11, 12) is partially covered with smoke along with polluted dust. Therefore it stands out in the BTD transect.

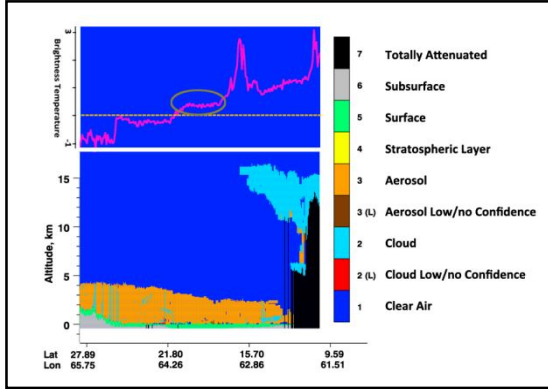


Fig. 19 : Comparison of BTD(11,12) with aerosol subtype (2008)

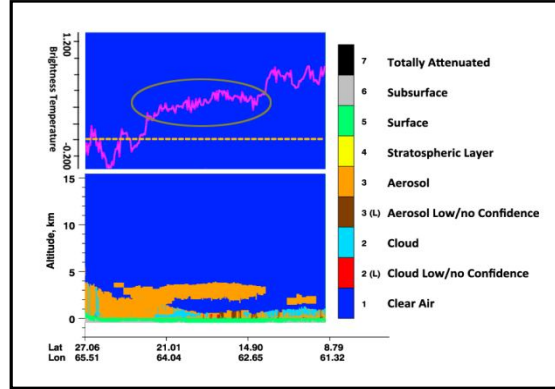


Fig. 20 : Comparison of BTD(11,12) with aerosol subtype (2011)

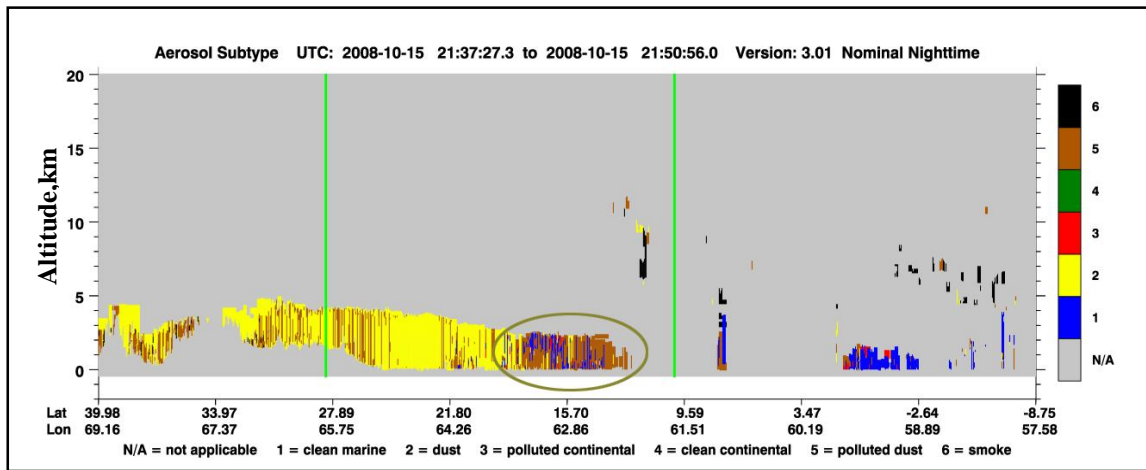


Fig. 21 : Aerosol subtype – presence of polluted dust (2008)

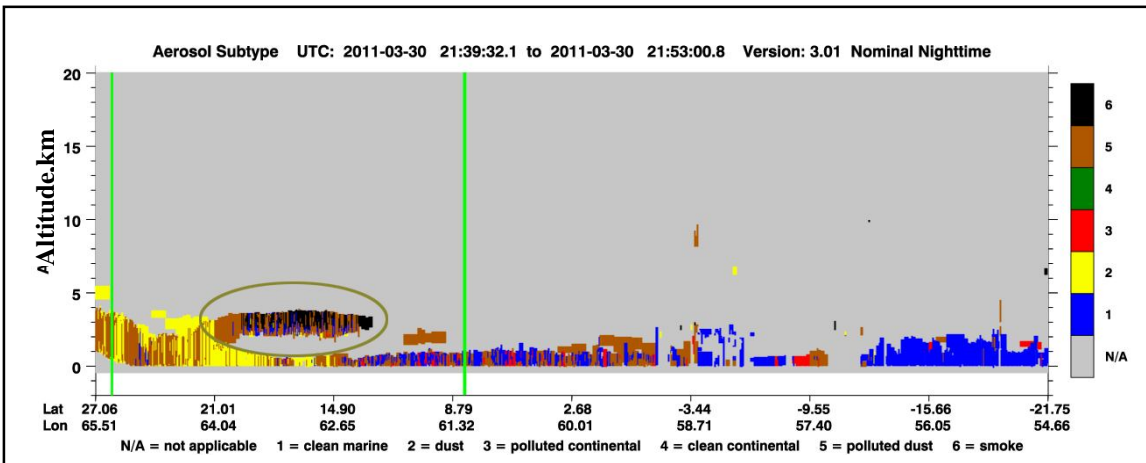


Fig. 22 : Aerosol subtype – presence of smoke (2011)

## **RESULTS AND DISCUSSION**

### **Dust detection**

As the spectral properties of dust aerosol are different from ground or sea, some predefined thresholds for various linear combinations can make dust clearly visible in the scene. NDDI and BTM (11,12) are effective measures techniques for dust detection over land and over ocean, respectively. All the algorithms discussed in this study are demonstrated by daytime images of Aqua and Terra MODIS only. However, the methods can be used with any other multi-channel satellite images with proper channels at (or close to) the channels used in this study. Presence of snow/ice also distresses dust signals heavily. Therefore these methods cannot be used in such regions. Cirrus clouds may produce some false positive results. Due to relatively weak aerosol signal and presence of bright land surface, thin and widely dispersed dust plumes may be missed in the detection process. For better classification accuracy, the results can be validated by CALIPSO LiDAR measurements.

### **Measurement and verification by CALIOP**

In both the events, the altitude of the dust is discovered to be 0-5 km above MSL (Mean Sea Level). The clouds on the other hand are at an altitude of 10-15 km above MSL. This information helps in largely analyzing the total attenuated backscatter profile for clouds and dust aerosols. Apart from this, the value of total attenuated backscatter at 532 nm for clouds is in range of  $6.5 \times 10^{-3}$  to  $1 \times 10^{-1}$ . The value of the same for dust particles are in range of  $1.5 \times 10^{-3}$  to  $2.5 \times 10^{-3}$ . For polluted dust particles, this value is slightly higher (from  $3.5 \times 10^{-3}$  to  $4 \times 10^{-3}$ ) compared to regular dust particles. When MODIS BTM (11, 12) profile is compared with Vertical Feature Mask of CALIOP, positive values of BTM for aerosol indicate presence of pollutants and smoke along with dust. The aerosol subtype profile shows the subclasses of aerosols. BTM is simple to calculate linear combination that highlights dust effectively. It is extremely suitable for dust detection over water. If characteristics of underlying ground surface are known, this can be the most simple and accurate method of determination. However,

this method may lead to confusing results in dust detection in presence of thin clouds. Reflectance values at 1.36  $\mu\text{m}$  can be used to screening out cirrus clouds. For dust detection over the land, positive NDDI values are an effective measure of dust. As the footprint of CALIOP is very narrow, it may miss the dust event by hundreds of kilometers at given time. Therefore the verification by CALIOP LiDAR measurements is not possible in such cases. As Aqua MODIS and CALIPSO are part of the A-train<sup>7-11</sup> there are high prospects of getting sufficient data for this type of comparison.

## **CONCLUSION**

It can be concluded from this study that multi-temporal satellite data is much efficient than ground measurements in detecting and tracing the path of the dust storm. The methods in this study have been evaluated by comparing values of linear combinations of MODIS channels with CALIOP measurements to minimize the misclassification. Although the methods minimize the false positive detection, thin layer of dust over ground may be missed. The threshold values for classifying a pixel as dusty pixel mentioned in this study may require adjustments depending on the event. These thresholds can be determined after verification by other methods of dust detection. Therefore the 'best' algorithm for detection of dust varies considerably and images should be examined on an event-by-event basis. This study is based on multi-spectral satellite imagery acquired during daytime only. Methods can be developed using absolute values of brightness temperature at 11- $\mu\text{m}$  and brightness temperature difference between 11 and 12  $\mu\text{m}$  wavelengths for dust detection in night time imagery. Also an intensity of the dust storm in an area can be quantified based on this brightness temperature difference. For future work, the findings of this study can be compared with meteorological parameters such as wind data to validate the actual movement of the dust storm.

## **ACKNOWLEDGEMENT**

We express our sincere gratitude to Director, National Institute of Oceanography for permitting us to publish this material. First author thankfully acknowledge to Dr. Anjana



Vyas of CEPT University, Ahmadabad for encouragement. First author carried out this study in NIO as summer intern student under 2<sup>nd</sup> author's guidance. MODIS data was accessed from <http://modis.gsfc.nasa.gov/>.

### REFERENCES

1. Liu Z., Omar A., Vaughan M., Hair J., Kittaka C., Hu Y., Powell K., Trepte C., Winker D., Hostetler C., Ferrare R. and Pierce R., CALIPSO LiDAR observations of the optical properties of Saharan dust : A case study of long-range transport, *J. Geophys. Res.*, **113**(7), 16, (2008).
2. Papadimas C.D., Hatzianastassiou N., Mihalopoulos N., Querol X. and Vardavas I., Spatial and temporal variability of aerosol properties over Mediterranean basin based on 6 years (2000–2006) MODIS data, *J. Geophys. Res.*, **113**(1), 12, (2008).
3. CALIPSO Data Products Catalog, [http://www-calipso.larc.nasa.gov/products/CALIPSO\\_DPC\\_Rev2x4.pdf](http://www-calipso.larc.nasa.gov/products/CALIPSO_DPC_Rev2x4.pdf), 26.08.13, (2007).
4. Miller S. D., An improved land/ocean dust enhancement applicable to MODIS, *Proc. 12th Conf. on Satell. Meteorol. Ocean.*, CD- ROM 3.2, American Meteorological Society, Long Beach, CA, (2003).
5. Tom X.P. Zhao, Steve Ackerman and Wei Guo, Dust and smoke detection for multi-channel imagers, *Rem. Sen.*, **2**(1), 2347-2368, (2010).
6. Ackerman S.A., Remote sensing aerosols using satellite infrared observations, *J. Geophys. Res.*, **102**(14), 17,069- 17,079, (2007).
7. A-train factsheet, formation flying : The afternoon A-train satellite constellation. Fs-2003-1-053-gsfc, NASA, [http://aqua.nasa.gov/doc/pubs/ATrain\\_Fact\\_sheet.pdf](http://aqua.nasa.gov/doc/pubs/ATrain_Fact_sheet.pdf), 08.11.13, (2003).
8. Singh Arti, Mishra Ayushman and Mishra Bhawana, Urban sprawl development and need assessment of landfills for waste disposal : A case study of Bilaspur municipal cooperation of Chhattisgarh, India, *J. Environ. Res. Develop.*, **7**(4A), 1718-1726, (2013).
9. Matin Shafigne, Behera Mukunda Dev and Mahapatra S.N., Criteria based approach to suggest alternative road network in part of Ladakh province through object based modeling : A GIS and remote sensing method, *J. Environ. Res. Develop.*, **7**(1), 88-98, (2012).
10. Kumar Mohit, Chauhan H.B., Rajawat A.S. and Ajai, Application of remote sensing and GIS techniques in understanding changes in mangrove cover in parts of Indus delta around Kori Creek, Gujarat, India, *J. Environ. Res. Develop.*, **7**(1A), 504-511, (2012).
11. Mishra Shalu, Spatial analysis of drainage network for ground water exploration in river basin using GIS and remote sensing techniques : A case study of tons river in Allahabad, India, *J. Environ. Res. Develop.*, **7**(3), 1316-1319, (2013).



*Environment should be put in the category of our national security. Defense of our resources is just as important as defense abroad. Otherwise what will remain there to defend?*

**Robert Redford**